



Published in final edited form as:

*Cryst Growth Des.* 2009 April 1; 9(4): 1806–1810. doi:10.1021/cg800990k.

## Measuring the nucleation rate of Lysozyme using microfluidics

Šeila Selimović, Yanwei Jia<sup>1</sup>, and Seth Fraden\*

Complex Fluids Group, Martin Fisher School of Physics, Brandeis University, Waltham, MA 02454

### Abstract

We employ the PhaseChip, a (poly)dimethylsiloxane (PDMS) microfluidic device, for statistical studies of protein crystal nucleation. The PhaseChip is designed to decouple nucleation and growth of protein crystals and so improve their yield and quality. Two layers of fluidic channels containing salt reservoirs and nanoliter-sized wells for protein drops in oil are separated by a thin PDMS membrane, which is permeable to water, but not to salt or macromolecules such as protein. We reversibly vary the supersaturation of protein inside the stored droplets by controlling the chemical potential of the reservoir. Lysozyme in the presence of sodium chloride is used as a model system. We determine the crystal nucleation rate as a function of protein supersaturation by counting the number of crystal nuclei per droplet, as demonstrated by Galkin and Vekilov.<sup>1</sup>

### Keywords

Microfluidics; PDMS; water permeation; high throughput; protein crystallization; phase diagram; nucleation

### Introduction

In this paper, we determine the nucleation rate of a protein crystal as a function of supersaturation at constant temperature using a microfluidic device previously described as the PhaseChip<sup>2,3</sup>. In brief, the PhaseChip is a two-layer microfluidic device composed entirely of PDMS. The top layer contains hundreds of droplets of protein solution stored in 2.8 nl wells and separated from each other by fluorinated oil. The second layer contains channels through which salt solutions flow. The two layers are separated by a thin membrane of PDMS, which is permeable to water, but not to protein or salt. Thus the second layer acts as a chemical potential reservoir. The difference in chemical potential of water inside the reservoir and inside a drop drives the flow of water across the membrane. Depending on the direction of this gradient, water flows either into the protein drops, thereby swelling them and lowering the solute concentration or out of the drops, therefore shrinking them and raising the solute concentration. Several independent reservoirs are fabricated on the chip, providing both spatial and temporal control over the protein concentration in the drops. Because the contents of the drops are isolated from each other by the fluorinated oil, each drop on the chip acts as an independent, sealed protein crystallization experiment.

One of the key attributes of the PhaseChip is that this design allows many different crystallization conditions to be tested simultaneously, since we can independently change the concentration in different sets of drops. More importantly, the concentrations of the solutes can be reversibly varied by changing the reservoir concentration allowing multiple cycles of supersaturation per sample without having to open the device. Other microfluidic systems that

\* Corresponding author. E-mail: fraden@brandeis.edu.

<sup>1</sup>Current address: Department of Biology, Brandeis University, Waltham, MA 02454

control the solute concentration, e.g. those developed by Ismagilov and Quake<sup>20,21</sup>, do not offer such wide range of control. The crystallization system developed by Quake utilizes free interface diffusion, and the Ismagilov approach uses microbatch droplets, however neither method is reversible. Crystallization methods that are based on temperature quenches, like in the case of Galkin and Vekilov are reversible, but the portions of the phase diagram accessible in a temperature quench are different than in a concentration quench.

We base our analysis of nucleation rates on the treatment employed by Galkin and Vekilov, 1,4. In their experiment, a temperature quench is used to change the protein supersaturation. The protein drops there are on the order of  $\mu\text{l}$  in volume, which is 100 times larger than in our case. The droplets are first cooled down to a nucleation temperature of  $12^{\circ}\text{C}$  to increase the supersaturation of protein. Next, the temperature is increased to  $20^{\circ}\text{C}$ , which lowers the protein supersaturation and is thus favorable for the growth of few large crystals. A comparison of our results with those of Galkin and Vekilov indicates a qualitative match, but also some notable quantitative differences. The error involved in the measurements presented here is large, but we propose simple ways of reducing it, promising significantly improved performance. Our results suggest that the PhaseChip design can be incrementally modified to develop a crystallization method that is easy to implement, offers convenient control of protein supersaturation, is high throughput, and uses small amounts of protein.

## Experiment

### Materials

The PhaseChip employed here houses over three hundred protein drops in individual wells. The protein solution is first prepared and filtered off-chip ( $0.2\ \mu\text{m}$  syringe filter, Corning, product number 431212) and contains  $17.5\ \text{mg/ml}$  Lysozyme (6x crystallized, Seikagaku),  $50\ \text{mM}$  NaAc at pH 4.5 and  $0.5\ \text{M}$  NaCl (Fisher). Then, protein drops are formed on-chip in a  $50\ \mu\text{m}$  nozzle flow-focusing geometry using fluorocarbon oil (Perfluoro compound FC43, Acros) with surfactant (12% w/w 1H,1H,2H,2H-Perfluoro-1-octanol, Fluka).<sup>2,3</sup> The surfactant lowers the surface tension and facilitates the drop formation. It also slows (though it does not prevent) drop coalescence. On-chip valves allow us to direct the flow to a waste line or, once drop formation is stabilized, to one of the four storage regions, each of which contains 62 drops on average. We expect the small number of drops to be a source of significant statistical error. In the experiment described in this paper, all aqueous drops have the same composition. The well volume is  $2.8\ \text{nl}$ ; the initial drop volume is usually smaller, on average  $1.4\ \text{nl}$  and varies between  $900\ \text{pl}$  and  $2.8\ \text{nl}$ . The complete storage region with all 300 wells is  $2\ \text{cm} \times 2\ \text{cm}$  in size. The protein drops are at all times surrounded by oil and chemically isolated from each other, because solutes do not pass between them. The storage channels are connected to a supply of oil so that as the drops swell and shrink oil flows into the device to compensate for the change in volume.

Underneath and separated from the wells by a water-permeable PDMS membrane ( $20\ \mu\text{m}$  thickness) are five independent reservoir channels. Each of them is connected to a different bottle of NaCl solution with  $0.5\ \text{m}$  long Tygon tubing ( $0.48\ \text{mm}$  ID).

### Experimental procedure

All 310 stored protein drops have the same initial conditions. During the loading of drops into storage wells all reservoir channels are filled with a  $0.5\ \text{M}$  NaCl solution, the same concentration of salt inside the drops. This prevents the concentration of solutes in the drops from changing before the experiment begins. After the drops are loaded, a  $4\ \text{M}$  NaCl solution is filled into all reservoirs and kept flowing for a quench time  $\Delta t$ , which varies for each reservoir. The device is placed on an automated movable microscope stage with a  $4\times$  objective lens with a resolution of  $10\ \mu\text{m}$ . We periodically record images of the protein drops, which allows us to

measure the size of the drops and thus changes in protein and solute concentrations and to record the appearance of crystals. The volume of the drop and shape of the wells are such that the drops take on a disk-like shape inside the storage wells, and the height of the drops is constant at all times. Hence, the change in drop volume only depends on the change in drop area, which we measure using automated image recognition software (NI Vision Assistant). Protein and salt concentrations in the drop at time  $t$  are then obtained from the drop area  $A(t)$ , the initial area  $A_0$ , and the known initial concentrations. The solubility values for Lysozyme in NaCl at pH 4.5 are taken from the literature.<sup>5</sup>

During the quench the drops shrink and both the protein and salt concentrations increase, two independent factors which increase the supersaturation. At a particular salt concentration, the supersaturation is calculated as  $C/C_s$ , where  $C$  is the protein concentration in the drop and  $C_s$  the equilibrium protein concentration (solubility) at this specified salt concentration. After this quench time, a 0.6M NaCl solution is introduced into the reservoir channels. The quench times are 4.0, 4.5, 5.0, 5.5, and 6.0 hours for reservoirs R1-R5, respectively. There are on average sixty-two drops exposed to each reservoir condition. As a consequence, each set of drops experiences a different level of supersaturation, depending on the quench time  $\Delta t$ , as shown in Figure 1.

The drops coupled to the first reservoir (R1) develop the lowest protein supersaturation, because they were exposed to a 4M NaCl solution for the least amount of time; conversely, the drops in exchange with R5 are the most supersaturated. Longer quench times result in higher protein supersaturations only when the quench times are shorter than the time for the drop and reservoir to equilibrate. The equilibration process is exponential with a time constant of 30 hours.<sup>2</sup>

In the work of Galkin and Vekilov<sup>1</sup>, temperature and thus supersaturation changes rapidly. Their experiment was designed such that drops were exposed to a single supersaturation level for different periods of time. In contrast, in our case, the supersaturation was continuously varied.<sup>5</sup>

## Results and discussion

Analysis of the drop images indicates that crystals grow during the low supersaturation period following the quench, so we conclude that all crystals have nucleated at the high supersaturation during the quench. This indicates that we have decoupled crystal nucleation from the growth process.

Figure 2 is a photograph of the PhaseChip showing protein drops containing crystals 118 hours after the start of the experiment. The majority of the drops above reservoir R1, corresponding to the lowest supersaturation, have no crystals. Conversely, all drops above reservoir R5 at the highest supersaturation have at least one and often more crystals. This observation is qualitative proof that a) the PhaseChip allows different crystallization conditions to be tested independently and simultaneously, and b) the supersaturation levels of protein inside every drop can be controlled.

Crystal nucleation is a stochastic phenomenon, so we evaluate our data and calculate the crystal nucleation rate by applying statistical methods. In accordance with the approach developed by Galkin and Vekilov<sup>1</sup> we count the number of drops containing  $m$  number of nuclei and normalize the distribution. We are interested in how well our data can be described by the Poisson distribution (Figure 3) and compute  $\chi^2$  values<sup>6</sup>

$$\chi^2 = \sum_m \frac{[N_{trial} P(m) - F(m)]^2}{N_{trial} P(m)}. \quad (1)$$

Here,  $N_{trial}$  is the number of drops exposed to one particular condition;  $F(m)$  are the measured frequencies and  $P(m)$  is the Poisson fit. The  $\chi^2$  values indicate poor agreement between our data and the Poisson law.<sup>7</sup> One reason is the small number of droplets per reservoir condition, making our system very sensitive to noise. Secondly, there are a few drops with eleven and twelve crystals each, while most drops at those conditions have three to four crystals. We believe that the formation of that many crystals per drop is at least partially due to heterogeneous nucleation, and as such it skews our homogeneous nucleation rate measurements.

We fit this data to the classical nucleation model,<sup>8,9,10,11</sup> in which the nucleation rate  $J$  [number of crystals / volume · time] can be expressed as

$$J = ACe^{\left(\frac{-B}{\sigma^2}\right)} \quad (2)$$

where  $\sigma = \ln\left(\frac{C}{C_s}\right)$ .

The parameter  $B$  is related to the surface tension  $\gamma$  of the nucleus,

$$B = \left(\frac{16\pi}{3}\right) \frac{\Omega^2 \gamma^3}{(k_b T)^3}, \quad (3)$$

and  $A$  is a measure of the kinetics of nucleation.<sup>12,15</sup> Analytic expressions for this prefactor vary considerably depending on the details of the theory, but in general  $A$  is also a function of supersaturation (and precipitant concentration). He and Attard<sup>13</sup> and Moody and Attard<sup>14</sup> have shown that the surface tension decreases with increasing supersaturation. In the range of supersaturations at which most crystals nucleate in our experiment ( $C/C_s = 24$  to  $55$ ), however, the surface tension varies little. Hence, we make the approximation that both quantities  $A$  and  $B$  are independent of the protein supersaturation. In our experiment, the drop volume  $V$  and therefore the concentration  $C$ , solubility  $C_s$  and nucleation rate  $J$  change with time. With these approximations we can calculate the number of crystals per drop as

$$N = \int_0^{\infty} V(t) A C(t) e^{\frac{-B}{\sigma(t)^2}} dt, \quad (4)$$

where we treat  $A$  and  $B$  as constants. We measure the average number of crystals,  $N_{exp}$ , per drop at times long after the quench.

We exploit this integral relationship by applying an optimization algorithm, based on Matlab's nonlinear least square fit (lsqnonlin). The algorithm has two parts: 1) It takes as inputs into equation (4) the supersaturation data as a function of time for each of the five quench profiles and 2) it computes the single values of  $A$  and  $B$  that give the best match between the calculated

mean number of crystals per drop  $N$  and the measured values  $N_{exp}$  for all five data sets simultaneously. Having obtained the best fit values for  $A$  and  $B$  we plot the extracted nucleation rate  $J(t)$  in Figure 4. The nucleation rate is highest for the profile with the longest quench time, since it obtains the largest supersaturation.

The fit gives  $A = 6.2 \cdot 10^5 \text{ mg}^{-1} \text{ s}^{-1}$  and  $B = 160$ . For comparison, the values of Galkin and Vekilov<sup>1</sup> are  $18 \text{ mg}^{-1} \text{ s}^{-1}$  and 65, respectively. The source and meaning of the large discrepancy in our values for  $A$  are unclear to us. The exponential term in the expression for  $J$ , however, is better understood and more important in characterizing the physical system. Consider equation (3), where  $\Omega$  is the protein molecular volume ( $3 \cdot 10^{-20} \text{ cm}^3$ ) and  $k_B T$  is  $4.14 \cdot 10^{-21} \text{ J}$ . We can then determine the surface tension  $\gamma$  of the critical cluster, again assuming that  $\gamma$  is independent of the supersaturation. Our calculation yields  $\gamma = 0.91 \text{ mJ/m}^2$ , which is in agreement with literature values for these crystallization conditions<sup>8</sup> (0.8 to 1.1  $\text{mJ/m}^2$ ), although somewhat larger than the value reported by Galkin and Vekilov (0.64  $\text{mJ/m}^2$ ). Another way to assess the validity of our numerical results is to plot the experimental values for  $N_{exp}$  as a function of quench time  $\Delta t$  and compare them to the values calculated from the optimized  $A$  and  $B$  constants (Figure 5). Data from five independent measurements of  $N_{exp}$  are fitted with two parameters ( $A, B$ ). The fact that the redundant theoretical and experimental results are in good agreement supports the model's validity.

Using the fitted values for  $A$  and  $B$  we can deduce the nucleation rate  $J$  at  $C_s = 5$  (the regime tested by Galkin and Vekilov). We find it is of the order of 1 crystal nuclei/ $\text{cm}^3 \text{ s}$  or less, which is several orders of magnitude smaller than reported by Galkin and Vekilov at the same supersaturations (Figure 6).

We suspect the following to be causes of the discrepancy between our results and those of Galkin and Vekilov.

1. We cannot exclude the possibility of heterogeneous nucleation, since some crystals appear to nucleate at the interface of the protein drop and the surrounding oil.
2. Contrary to the experiment of Galkin and Vekilov, we change the protein supersaturation by changing the size of the protein drop and, by extension, the protein concentration. As the drops are quenched to a volume  $\frac{1}{3}$  to  $\frac{1}{4}$  of the original volume, they begin to pin on the wall of the storage chamber; in the future a judicious choice of surfactant can reduce this problem<sup>16</sup>. The drops did not shrink uniformly and a thin film of protein remained on the PDMS wall. Without the use of fluorescently labeled protein it is not possible to determine the extent of this film and how much protein remains in the aqueous drop. This is a cause of error in the measurement of a) the protein supersaturation at which the crystals nucleate and b) the drop volume at those supersaturations. We can experimentally probe the extent of this error and thus the discrepancy between our and Galkin-Vekilov results by using different surfactants and varying their concentrations.
3. The salt concentration in our experiment is not constant, while in the case of Galkin and Vekilov it remains at 2.5% throughout the duration of the experiment. This makes it difficult to compare our respective results.
4. The supersaturation in our experiment is constantly changing during the quench. We assume that most crystals nucleate at the highest supersaturations ( $\pm 10\%$ ), but the time spent in this regime is short (on average 1 hour). Consequently, some nuclei may not grow large enough and will melt during the subsequent low supersaturation period. Therefore, we expect the mean number of crystals  $N_{exp}$  and hence the nucleation rate to be small compared to that of Galkin and Vekilov, where the high supersaturation

is maintained for up to twelve hours. In the future, we will use fluorescently labeled protein to obtain more information about the origin and evolution of crystals.

5. Lastly, our assumption that the nucleus surface tension and the constants  $A$  and  $B$  are independent of the protein solubility in the range of interest could be a source of error. For example, a 10% decrease in surface tension results in an increase in nucleation rate of up to  $10^6$  orders of magnitude. In principle the surface tension of the protein crystal-solution interface should be measured independently.

## Conclusion

We have shown that the PhaseChip is a promising device for protein crystallization, in particular for optimization of crystallization conditions. Varying the quench depth (concentration) of protein drops on-chip is a practical way to control protein supersaturation levels. The PhaseChip makes this process as convenient as changing the temperature of the test solution through the exchange of water between the protein drop and reservoir. Controlling the protein concentration in specific ways can be used to decouple nucleation from growth, as we have demonstrated by the observation that the number of crystals per drop is strongly correlated with the degree of supersaturation. This approach can be utilized to both screen hundreds of crystallization conditions simultaneously and optimize the crystal growth at a few selected conditions. This device can also be easily combined with a temperature stage, as suggested by Laval et al.<sup>17</sup> in order to increase the number of explored crystallization pathways.

The calculated values of nucleation parameters such as the nucleation rate and surface tension of critical nuclei in our experiment are somewhat higher than those found by Galkin and Vekilov, but still within the range of literature results.<sup>1,2,3,18</sup> We suggest that this discrepancy comes chiefly from the experimental method applied, where the supersaturation during the quench is not constant, and from the approximation of constant surface tension employed during analysis.

Future experiments will rely on the use of a better surfactant to avoid protein film formation. We will also use fluorescently labeled protein and dynamic light scattering to detect crystals earlier in order to better analyze crystallogensis. Additionally, using non-confined spherical drops in contrast to disk-shaped confined drops will minimize protein contact with PDMS, which should lower the heterogeneous nucleation rate. Such a device could contain thousands instead of hundreds of drops and so significantly improve our statistics. We also envision modifying the discrete concentration gradient<sup>19</sup> employed in the current PhaseChip reservoir into a continuous gradient and using it in tandem with a temperature gradient stage, to greatly increase the number of crystallization conditions that can be screened at the same time.

## Acknowledgments

The authors would like to acknowledge funding from National Institutes of Health NIH-NIGMS, STTR R41 GM083482-01. We acknowledge Jung-uk Shim's work developing the microfluidic device and thank Michael Heymann for assistance with the numerical model and Frédéric Gobeaux for helpful discussions.

## References

1. Galkin O, Vekilov PG. *J Phys Chem B* 1999;103:10965–10971.
2. Shim JU, Cristobal G, Link DR, Thorsen T, Jia Y, Piattelli K, Fraden S. *J Am Chem Soc* 2007;129:8825–8835. [PubMed: 17580868]
3. Shim JU, Cristobal G, Link DR, Thorsen T, Fraden S. *Crystal Growth & Design* 2007;7:2192–2194. [PubMed: 19590751]
4. Vekilov PG, Galkin O. *Colloids and Surfaces A: Physicochem Eng Aspects* 2003;215:125–130.

5. Howard SB, Twigg PJ, Baird JK, Meehan EJ. *Journal of Crystal Growth* 1988;90:94–104.
6. Young, HD. *Statistical Treatment of Experimental Data*. McGraw-Hill; New York: 1962.
7. Fisher, RF.; Yates, F., editors. *Statistical tables for biological, agricultural, and medical research*. Oliver and Boyd; Edinburgh: 1963.
8. Vekilov PG, Monaco LA, Thomas BR, Stojanoff V, Rosenberger F. *Acta Crystallogr Sect D* 1996;52:785–798. [PubMed: 15299643]
9. Debenedetti, PG. *Metastable Liquids Concepts and Principles*. Princeton University Press; Princeton: 1996.
10. Kashchiev D. *J Chem Phys* 1982;76(10):5098–5102.
11. Oxtoby DW, Kashchiev D. *J Chem Phys* 1994;100(10):7665–7671.
12. Oxtoby DW, Evans R. *J Chem Phys* 1988;12:7521–7530.
13. He S, Attard P. *Phys Chem Chem Phys* 2005;7:2928–2935. [PubMed: 16189613]
14. Moody MP, Attard P. *Phys Rev Lett* 2003;91:56104.
15. Garcia-Ruiz JM. *Journal of Structural Biology* 2003;142:22–31. [PubMed: 12718916]
16. Boxshall K, et al. *Surf Interface Anal* 2006;38:198–201.
17. Laval P, Salmon JB, Joanicot M. *J Crystal Growth* 2007;303:622–628.
18. Zukoski CF, Kulkarni AM, Dixit NM. *Colloids and Surfaces A: Physicochem Eng Aspects* 2003;215:137–140.
19. Jeon NL, Dertinger SKW, Chiu DT, Choi IS, Stroock AD, Whitesides GM. *Langmuir* 2000;16:8311–8316.
20. Li L, Mustafi D, Fu Q, Tereshko V, Chen D, Tice J, Ismagilov R. *PNAS* 2006;103:19243–19248. [PubMed: 17159147]
21. Hansen C, Quake S. *Current Opinion in Structural Biology* 2003;13:538–544. [PubMed: 14568607]

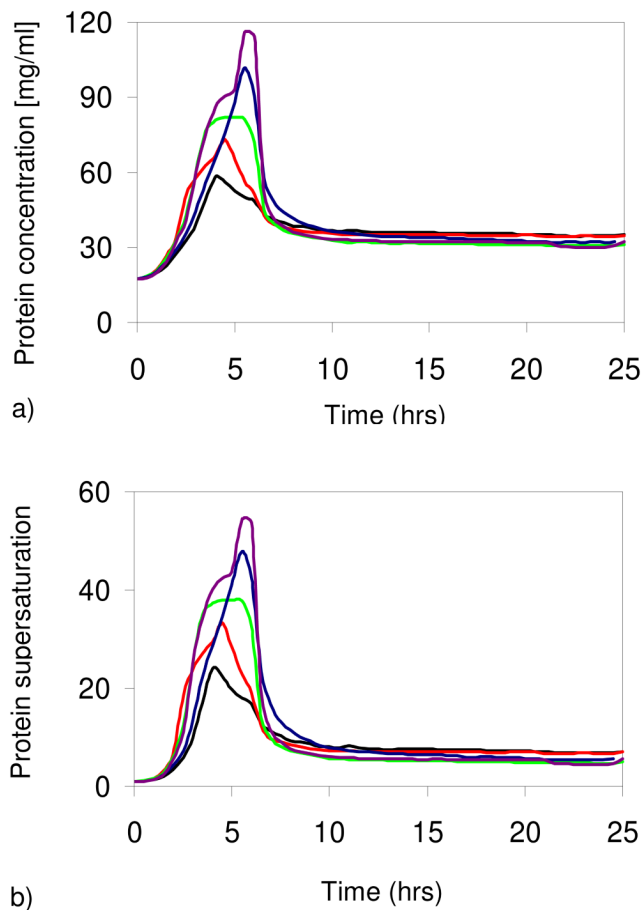


**Figure 1.** (a) Protein concentration ( $C$ ) and (b) supersaturation ( $C/C_s$ ) in five sets of droplets with 4M NaCl in the reservoir. Black lines: reservoir 1 (R1) with quench time  $\Delta t = 4$  h. Red: R2 with  $\Delta t = 4.5$  h. Green: R3 with  $\Delta t = 5$  h. Blue: R4 with  $\Delta t = 5.5$  h. Purple: R5 with  $\Delta t = 6$  h. (Online in color.)



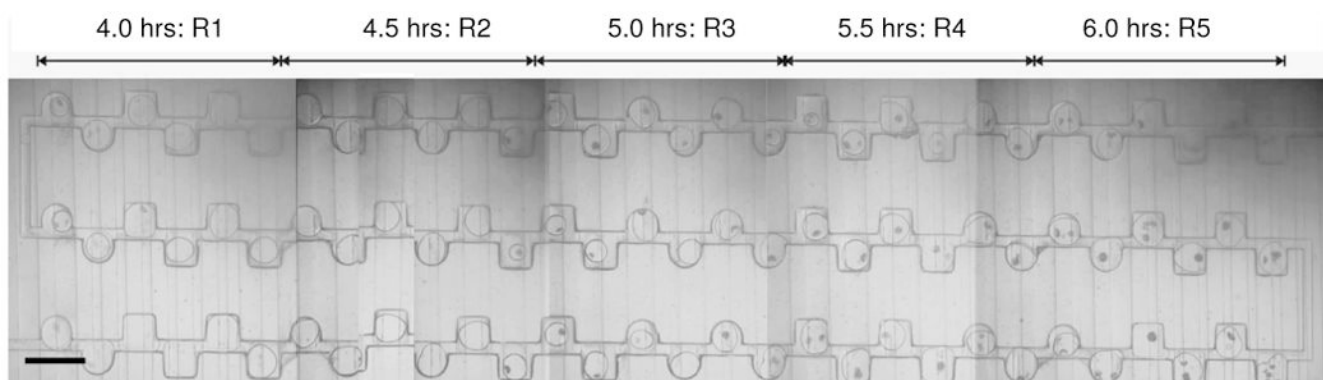


**Figure 2.**

Protein crystals obtained on the PhaseChip for different quench times. On the left side of the device, the quench time is shortest (4 hours) and hence the supersaturation is lowest, so only few crystals nucleate. On the right side, the quench time is longest (6 hours), the supersaturation is largest and there is one or more crystals per drop. The scale bar is 500  $\mu\text{m}$ .

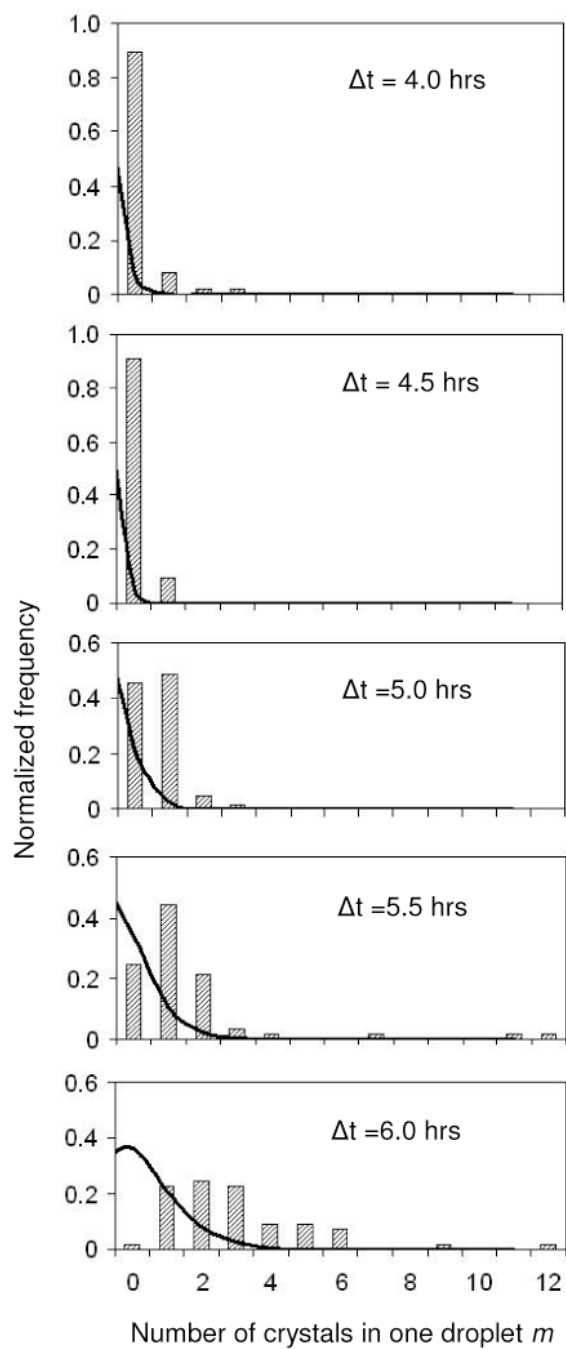


**Figure 3.** Distribution of  $m$  Lysozyme crystal nuclei per droplet for different quench times. The shorter the quench time, the lower the protein supersaturation inside the drop and the fewer crystals nucleate.

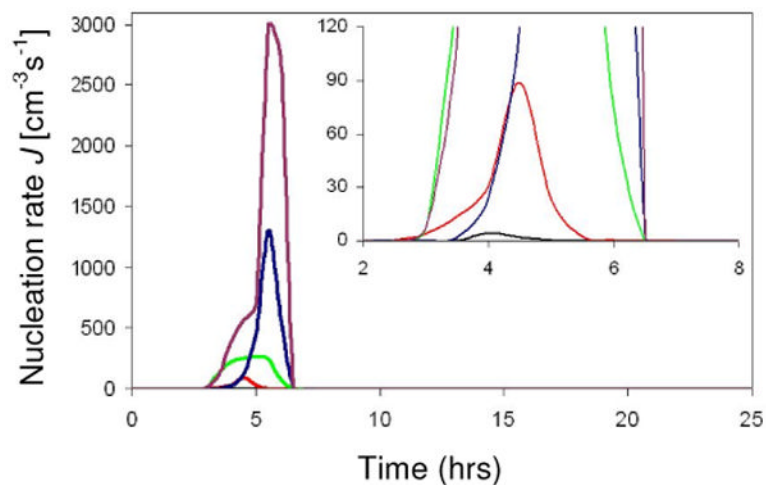


**Figure 4.** Deduced nucleation rate  $J$  of Lysozyme in presence of 0.5M NaCl and 0.05M NaAc at pH 4.5, as a function of time. The inset is a close-up of the main graph. The different curves describe  $J$  for different quench profiles. (Online in color.)

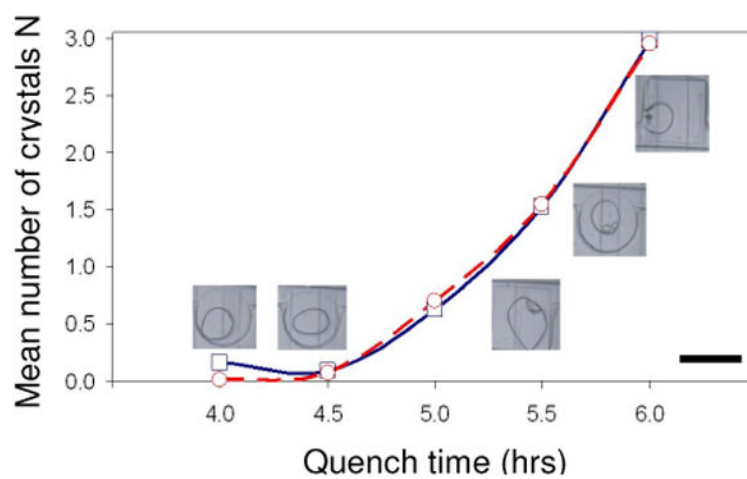


**Figure 5.** Mean number of crystals  $N$  per drop as a function of quench time in hours: Measured values (blue squares) and calculated results (red circles). The lines are a guide for the eye. The images show typical drops from each quench profile. The scale bar is 300  $\mu\text{m}$ . (Online in color.)

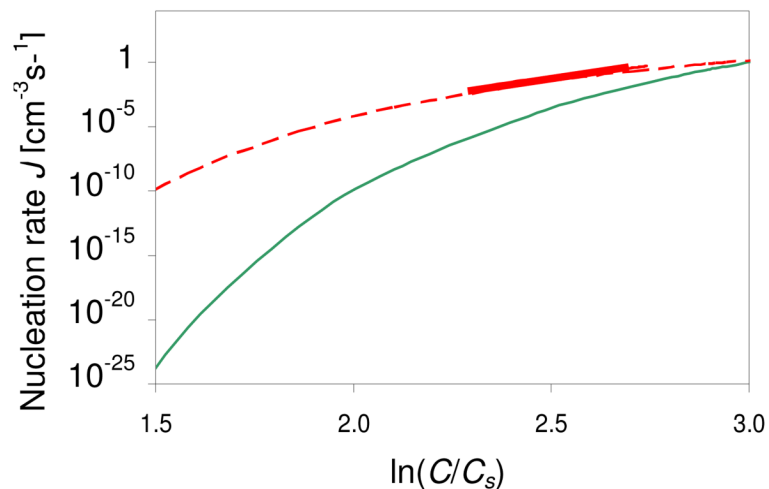


**Figure 6.**

Crystal nucleation rate  $J$  as a function of supersaturation. Solid (thin) green curve: nucleation rates calculated using our fitting parameters  $A = 6.2 \cdot 10^5 \text{ mg}^{-1} \text{ s}^{-1}$  and  $B = 160$  (extracted from a crystallization experiment with initially 3.5% NaCl), for protein solubility  $C_s = 5 \text{ mg/ml}$  and a range of protein concentrations (20 mg/ml to 100 mg/ml). Dashed red curve: nucleation rates calculated using the fitting constants of Galkin and Vekilov ( $A = 18 \text{ mg}^{-1} \text{ s}^{-1}$  and  $B = 65$ , extracted from a crystallization experiment with 2.5% NaCl). Solid (thick) red curve: experimental data of Galkin and Vekilov at  $C_s = 5$ . (Online in color.)